

Article

Porcospino Flex: A Bio-Inspired Single-Track Robot with a 3D-Printed, Flexible, Compliant Vertebral Column

Shahab Edin Nodehi ¹, Luca Bruzzone ^{2,*}, Mohammadreza Lalegani Dezaki ³, Ali Zolfagharian ⁴
and Mahdi Bodaghi ^{3,*}

¹ The BioRobotics Institute, Scuola Superiore Sant'Anna, 56127 Pisa, Italy; shahabedin.nodehi@santannapisa.it

² Department of Mechanical, Energy, Management and Transport Engineering (DIME), University of Genoa, 16145 Genoa, Italy

³ Department of Engineering, Nottingham Trent University, Nottingham NG11 8NS, UK; mohammadreza.laleganidezaki2021@my.ntu.ac.uk

⁴ School of Engineering, Deakin University, Geelong, VIC 3216, Australia; a.zolfagharian@deakin.edu.au

* Correspondence: luca.bruzzone@unige.it (L.B.); mahdi.bodaghi@ntu.ac.uk (M.B.)

Abstract: This paper is focused on the design and development of the Porcospino Flex, a single-track robot inspired by nature and featuring a meta-material structure. In the earlier version of the Porcospino, the main body was composed of a chain of vertebrae and two end sections linked by flexible joints, but the excessive use of materials in 3D printing and the resulting weight of the robot posed challenges, ultimately leading to a decrease in its overall efficiency and performance. The Porcospino Flex is manufactured through the fused deposition modeling process using acrylonitrile butadiene styrene and thermoplastic polyurethane, featuring a singular meta-material structure vertebral column. The adoption of a lattice structure in the main body of the Porcospino Flex leads to a substantial increase in performance, reducing its weight from 4200 g to 3600 g. Furthermore, the decrease in weight leads to a reduction in material usage and waste, making a substantial contribution to the sustainability of the robot. The discussion focuses on the testing results of the Porcospino Flex prototype, highlighting the enhancements observed compared to its prior version.

Keywords: snake robot; worm robot; tracked locomotion; single-track; compliant mechanism; meta-material structure



Citation: Nodehi, S.E.; Bruzzone, L.; Lalegani Dezaki, M.; Zolfagharian, A.; Bodaghi, M. Porcospino Flex: A Bio-Inspired Single-Track Robot with a 3D-Printed, Flexible, Compliant Vertebral Column. *Robotics* **2024**, *13*, 76. <https://doi.org/10.3390/robotics13050076>

Academic Editors: Cecilia García Cena, Carlos Rengifo-Rodas and Jose Baca

Received: 5 April 2024

Revised: 4 May 2024

Accepted: 10 May 2024

Published: 13 May 2024



Copyright: © 2024 by the authors. Licensee MDPI, Basel, Switzerland. This article is an open access article distributed under the terms and conditions of the Creative Commons Attribution (CC BY) license (<https://creativecommons.org/licenses/by/4.0/>).

1. Introduction

There has been a notable surge in the growth of service robots. Navigating ground mobile robots effectively in both structured and unstructured environments poses a significant challenge for the future [1]. The versatility of ground mobile robots makes them suitable for a wide range of applications, including agriculture, planetary exploration, military operations, demining, counter-terrorism, surveillance, and reconnaissance in hazardous conditions [2]. Going beyond their commercial use in indoor industrial settings, ground mobile robots have the potential to significantly impact many different fields.

The design of ground mobile robots is profoundly interdisciplinary, involving elements of mechanics, vision, cognition, and navigation. There are various locomotion principles for ground mobile robots, including wheeled [3,4], legged [5,6], tracked [7,8], and hybrid designs [9–12]. Moreover, other bio-inspired locomotion principles are proposed in the scientific literature [13–15]. Each design choice involves a trade-off between various factors, including their maximum speed, obstacle crossing ability, step/stair climbing ability, slope climbing ability, walking capability on soft terrain, walking capability on uneven terrain, energy efficiency, mechanical complexity, control complexity, and technology readiness [2].

Tracked robots have excellent motion capabilities on uneven and yielding terrain. This is due to their large contact surface with the ground, which provides greater stability and traction compared to other design options, even if they are generally slower and less

efficient than wheeled robots [16]. To conjugate the performance on soft grounds and the capability of moving in narrow spaces, researchers have proposed snake-like tracked robots, composed of a series of tracked modules capable of adapting to the terrain irregularities, which represent a promising solution for inspection and surveillance tasks in challenging environments [17,18].

An alternative approach to designing robots for inspecting confined spaces is to outfit a worm-like robot with a solitary peripheral track [19]. An example is the Flexible Mono-Tread Mobile Track (FMT), with steering and maneuverability capabilities [20]. Another single-track robot is the Reconfigurable Continuous Track Robot (RCTR), which can actively bend its column to overcome obstacles but has poor steering capabilities [21]. A third example of a single-track robot is the Porcospino, characterized by track modules with elastic spines to enhance its obstacle-crossing ability [22].

Modern manufacturing has undergone a radical change because of the incorporation of robotic and 3D printing technology. The design iteration process has been simplified and has never been possible with the level of customization made possible by three-dimensional (3D) printing's rapid prototype production and ability to build complicated shapes [23]. Additionally, this technology has greatly decreased material waste, which is consistent with sustainable production methods [24]. In the meantime, robotic parts have become highly accurate workhorses that can do repetitive operations with unmatched precision. Their agility and unwavering work ethic have resulted in significant gains in efficiency and output. Furthermore, robots perform exceptionally well in dangerous settings, reducing the dangers to human workers and enhancing general workplace safety [25].

By integrating compliant mechanisms and meta-materials, the design of a bio-inspired snake-like robot can undergo substantial enhancements. Recently, improvements in additive manufacturing (AM) technologies, also known as 3D printing, have made it possible to make meta-structures with 2D or 3D lattices that can deform in both elastic and elastoplastic ways [26]. Currently, there is an ongoing demand to decrease the weight of structures while preserving their primary attributes and even improving them. One prevalent approach to accomplishing these objectives involves the development of lattices or meta-structures [27]. Ref. [28] examined the unique mechanical properties of origami tubes and provided a novel way of linking them in a zipper-like fashion. Thin sheets in tension, compression, and shear were used in these assemblies for any deformation mode that deviates from the recommended deployment order. Stacking and combining origami tubes into different cellular structures increased the mechanical qualities and adaptability of the robot. Subsequent developments and enhancements of this methodology investigated geometric arrangements to augment stiffness-to-weight ratios, influence energy dissipation, and augment mechanical characteristics. Also, there are other ways to improve the maneuverability and performance of robots. Ref. [29] introduced a 3D-topology-optimization-based approach for multi-axis flexure joint design. Utilizing a multi-objective algorithm, the optimization considered torsional stiffness and rotational flexibility across different axes of the joint structure. Artificial spring elements were incorporated to ensure a balanced stress distribution.

Meta-materials are often defined as engineered materials possessing properties that are uncommon or absent in natural materials. They are typically structured with repetitive cellular geometries [30]. Meta-materials are used in robotics in a variety of ways [31]. They can be designed not only to obtain specific mechanical features but also to have specific responses to electromagnetic radiation, for example, for microwave filters, cloaking devices, and superlens applications [32]. Meta-structures are widely used to achieve enhanced performance and functionalities in a variety of fields, including photonics [33] and acoustics [34].

By using them, lightweight and highly strong components may be made, improving the overall performance and efficiency of robotic systems. As an instance of this, Dikici et al. designed a soft, pneumatic crawling robot utilizing a meta-material structure and fused deposition modeling (FDM) process, enabling it to navigate through pipes [35]. The

lightweight robot exhibits substantial expansion and deformation capabilities, thanks to its lattice structure, resulting in high performance. Focusing on mechanics, meta-structures are designed to exhibit specific mechanical properties, such as high stiffness, low density, and low thermal conductivity [36]. This leads to the creation of new materials for various applications, such as structural and vibration control [37]. Therefore, incorporating meta-structures into robots aids in minimizing material usage, reducing waste, and decreasing the weight of the robot.

This paper aims to create and advance a bio-inspired, single-track robot known as the Porcospino Flex. The research goals include reducing of the robot's weight, minimizing material usage, enhancing efficiency, and improving maneuverability. These enhancements contribute to a greener design, resulting in a more sustainable and efficiently functioning robot. Thus, the vertebral column of the Porcospino [22] is reinforced and developed with a lattice structure to decrease the overall weight of the robot, subsequently enhancing its energy efficiency. The Porcospino Flex is fabricated and developed using FDM 3D printing technology. The robot's structure is printed using thermoplastic polyurethane (TPU) and acrylonitrile butadiene styrene (ABS) materials. The lightweight meta-material core enables excellent structural compliance in the robot, enhancing maneuverability at higher speeds. The design's lower stiffness provides the advantage of allowing the robot's body to bend up to 120 degrees. Additionally, the production time decreases substantially due to the reduction of the number of printed pieces from 40 to a continuous vertebral column. The details of robot development are thoroughly examined to investigate its performance in the following sections.

2. The Functional Design of the Porcospino Flex

Millipedes (Figure 1, left) are distinguished by a segmented body structure consisting of several repeating units or segments, joined by movable joints, which confer remarkable flexibility and adaptation in negotiating challenging terrain [38]. They move in unison by contracting and extending these segments one after the other, using wave-like motion patterns that propel them remarkably well. Due to their unusual gait, millipedes can traverse a variety of situations by swaying their bodies and utilizing traction and friction to move forward while maintaining stability.



Figure 1. Sources of inspiration: millipede (left); porcupine (right).

On the other hand, the characteristic feature of porcupines (Figure 1, right) is a coat of sharp, barbed quills covering their bodies, serving as a robust barrier against predators [39]. Because of the weight and bulkiness of their quills, they must walk slowly and deliberately to navigate their surroundings. This requires cautious and methodical strides. Due to their distinctive way of moving, porcupines must balance carefully and make strategic motions to avoid injuring themselves with their protective quills while navigating different types of terrain.

The Porcospino Flex has been conceived, drawing inspiration from millipedes and porcupines. The design process begins with the creation and development of each component. These parts are meticulously designed and assembled to minimize errors and material waste. The 3D schematic of the Porcospino Flex robot is illustrated in Figure 2, measuring 670 mm in length, 165 mm in width, and 145 mm in height. The vertebral column of the Porcospino Flex (see Figure 3) is composed of a unified single body with 16 sections. A 2D lattice structure is designed to work as the main body of the robot. Between adjacent sections, there are fifteen 8° grooves, which enable the entire column to bend at 120 degrees. This compliant vertebral column, with low stiffness for the yaw rotation, allows for lateral flexion for steering with low energy consumption. The design is carefully chosen to prevent collisions with other components while also minimizing weight. Additionally, it needs to be sufficiently rigid to prevent buckling due to the placement of the battery, motor drivers, and control unit. The body dimensions are 440 mm in length, and 120 mm in width, with a thickness of 10 mm. As a result, the main body is rigid enough to maintain its structural integrity, yet it possesses flexibility in two directions, providing the robot with greater freedom of movement. This particular design is selected to enhance the stability and rigidity of the robot while still maintaining its mechanical properties and performance. Achieving this design involved a process of trial and error, considering both component assembly and flexibility requirements. The central portion of the 2D design must possess sufficient rigidity to accommodate the electrical components effectively. Consequently, this design contributes to the overall stability of the robot. Additionally, the inclusion of lateral supports during assembly complicates the adoption of alternative designs.

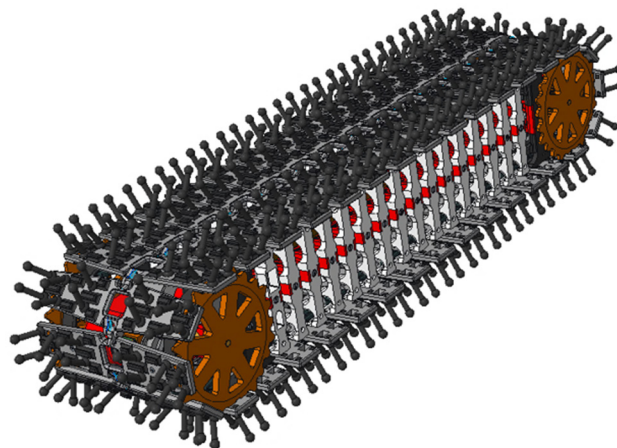


Figure 2. A 3D schematic view of the Porcospino Flex.

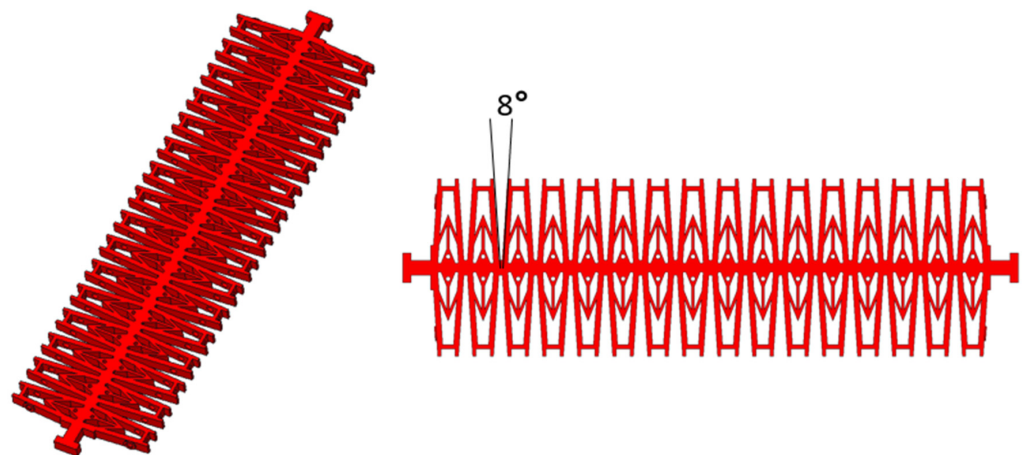


Figure 3. The design of vertebral column of the Porcospino Flex.

The robot has symmetrical end modules that are symmetric in shape both with respect to the front–rear and the up–down planes (see Figure 4). Figure 4 shows the location of the control unit (CU), batteries (Bs), and motor drivers (MDs) along the vertebral column, where additional sensors for specific tasks can be placed. Each end module consists of two actuators, a track actuator (TA) and a steering actuator (SA). The DC motor TA controls the movement of the two sprockets (TSs), while the gearmotor SA is linked to the winch (W), responsible for driving the lateral flexion of the column by pulling the rope (R). The rope threads through the holes (Hs) in the vertebrae (refer to Figure 5) and is secured at one end to the winch and at the other end to the opposing end module. To execute lateral steering, the robot pulls the rope on the side towards the center of the intended turn while simultaneously releasing the opposite rope.

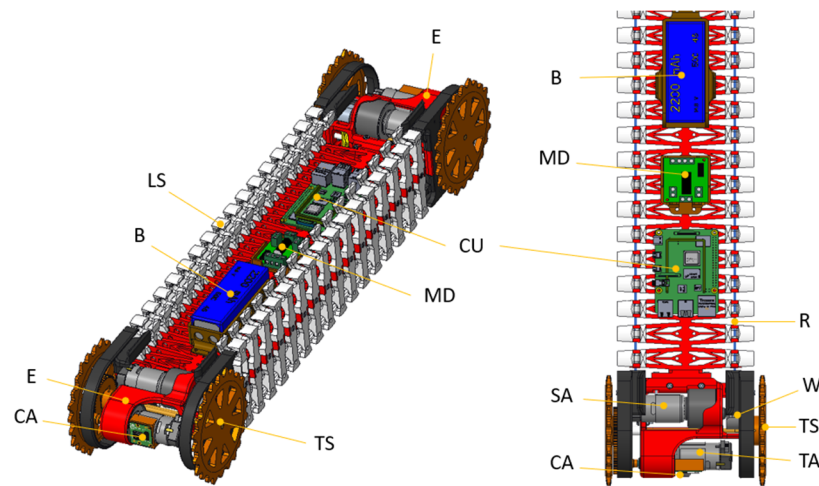


Figure 4. The internal components of the Porcospino Flex.

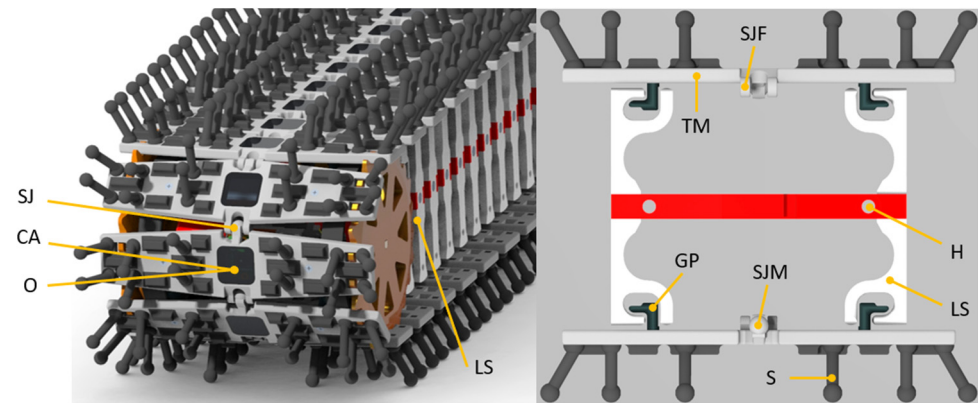


Figure 5. The details of the track modules and guidance system.

Moreover, Figure 5 depicts a closeup of the track modules. They are distinguished by center apertures (see Figure 5, O) that permit an intermittent view through the two cameras installed on the end modules (see Figures 4 and 5, CAs). The lateral supports attached to each vertebra (see Figures 4 and 5, LSs) and the guiding pegs attached to the track modules (see Figure 5, GP) ensure the guidance of the tracks (see Figure 5, TMs) along the vertebral column. Spherical joints (see Figure 5, SJs) are used to link the track modules. The male and female spherical parts of the spherical joint are created by printing precisely on the tracked module, and the female part’s elasticity makes it possible to assemble the joint. The track spines (Figures 4 and 5, Ss) and the guiding pegs of the track modules (see Figure 5, GPs), on the other hand, are printed separately and connected by interference.

The camera vision is operational only when it is aligned with a track opening. With a track spacing of 40 mm and a standard robot speed of 0.1 m per second, the camera's perspective can be refreshed at a rate of 2.5 frames per second. Although this may not be considered to be high, it is adequate for directing the robot, given its relatively slow pace. Therefore, this constraint is not especially significant for regular inspection tasks; in any event, the robot can pause for ongoing monitoring.

3. The Embodiment Design of the Vertebral Column

The vertebral column can perform a maximum 120° yaw flexion for steering with an elastic return force due to its compliant realization; on the contrary, the spherical joints that connect the track modules have no elastic return force, and the track shape is guided by the contact between the guiding pegs (CPs) and the lateral supports (LSs) (Figure 5). The vertebral structure is not compliant only in the yaw direction for active steering but also in the pitch and roll directions for its passive adaptation to ground unevenness.

The proposed compliant body design, shown in Figure 3, is realized in a TPU 95A elastic material and connected to the end modules of the robot. The grooves in the body define the maximum relative yaw motion (8° between two adjacent vertebrae), while they have a minimal effect on pitch and roll flexions. This means that they can passively adapt to the terrain profile through passive retroflexion and torsion. This design helps to increase the robot's flexibility and versatility, making it capable of navigating through a range of environments with ease. The use of a TPU 95A material provides the robot with the required durability and structural resistance.

The continuous, compliant vertebral column of the Porcospino Flex offers several advantages over the previous version of the Porcospino [22], which had separate vertebral units connected by compliant joints. These advantages include:

- The weight being reduced by 650 g (total weight of the robot is 3.6 kg instead of 4.2 kg);
- The production speed being increased and the cost reduced due to the elimination of the assembly process;
- The shock resistance being enhanced due to the softer main body structure.

The reduction in weight can lead to notable improvements in agility and maneuverability, especially in scenarios where precise movements and navigation through tight spaces are required. Additionally, the decrease in weight contributes to the robot's sustainability by reducing material usage and waste, aligning with the growing emphasis on eco-friendly designs in robotics. Furthermore, while the weight reduction alone may not completely overhaul the capabilities of the old robot, it serves as one aspect of a broader optimization effort that likely includes improvements in structural design, material selection, and overall performance. Thus, while reducing weight may not be the sole solution for enhancing the robot's capabilities, it undoubtedly plays a crucial role in its overall improvement and merits further consideration and elaboration.

To better understand the structural behavior of the vertebral column, a finite element modeling (FEM) model is created to analyze the displacements and von Mises stresses that occur during bending. In analyzing the robot's main body through the FEM, the simulation was executed using PTC Creo Simulate 7, a robust software tailored for structural analyses. Primarily, a comprehensive 3D model of the body was created, and every aspect of its geometry was precisely defined. The simulation utilized the flexible material TPU 95A with the goal of accurately simulating the bending behavior of the main robot's body. Tetrahedral and hexahedral components were used in tandem with a careful meshing technique to achieve this. In order to maintain simulation accuracy while accurately capturing the body's complex shape, this mesh arrangement was used. Throughout the model, the mesh size was carefully adjusted, using smaller elements, particularly around crucial stress zones, including the body's two ends, to accurately depict the distribution of stress while maintaining computational efficiency. An accurate assessment of the body's flexural behavior was made possible by the strategic decision to include the center of the body as a constraint inside the simulation. This decision resembled the situation in which the

body's center remained clamped or fixed, consequently providing a reliable representation of real-world events.

Figure 6 shows the detail of the FEM mesh of the vertebral column, characterized by tetrahedral elements with a maximum size of 2 mm. In the FEM analysis, the displacements of the central section of the vertebral column are constrained, and forces are applied to the end modules, simulating the action of the active steering rope on the internal side of the turn. Figures 7 and 8 show the distributions of the von Mises stress [kPa] and displacement [mm] of different rope tensions (4, 5, and 6 N), respectively. As Figure 7 shows, the most stressed zones are the restrictions close to the grooves, as expected.

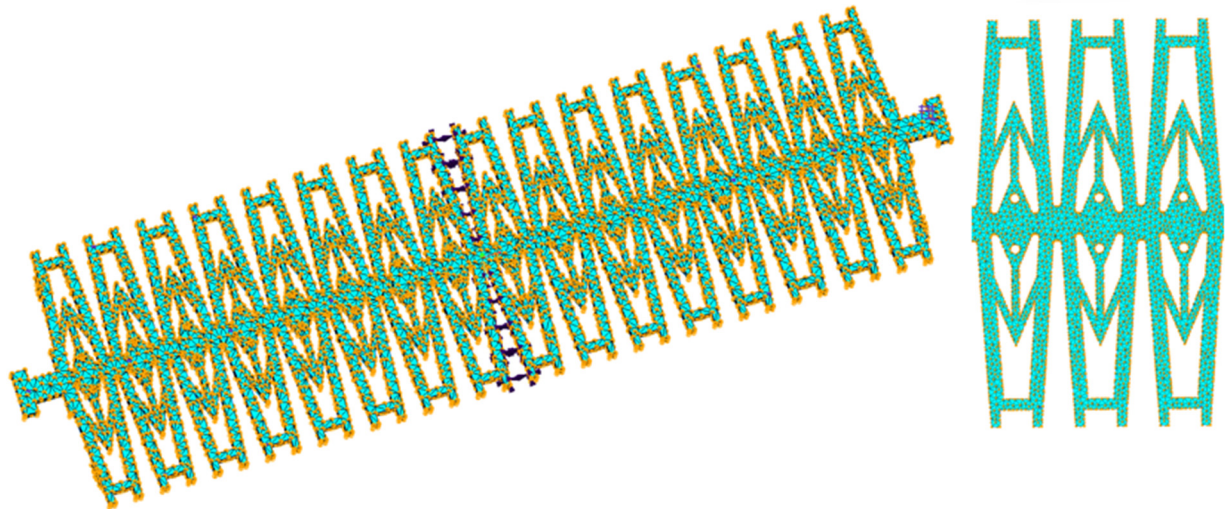


Figure 6. A FEM mesh model of the vertebral column.

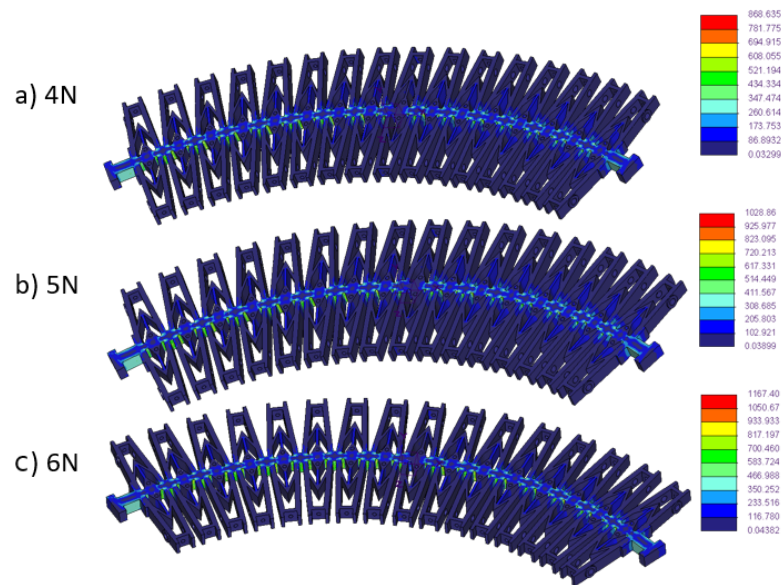


Figure 7. The von Mises stress [kPa] of different rope tensions (4, 5, and 6 N).

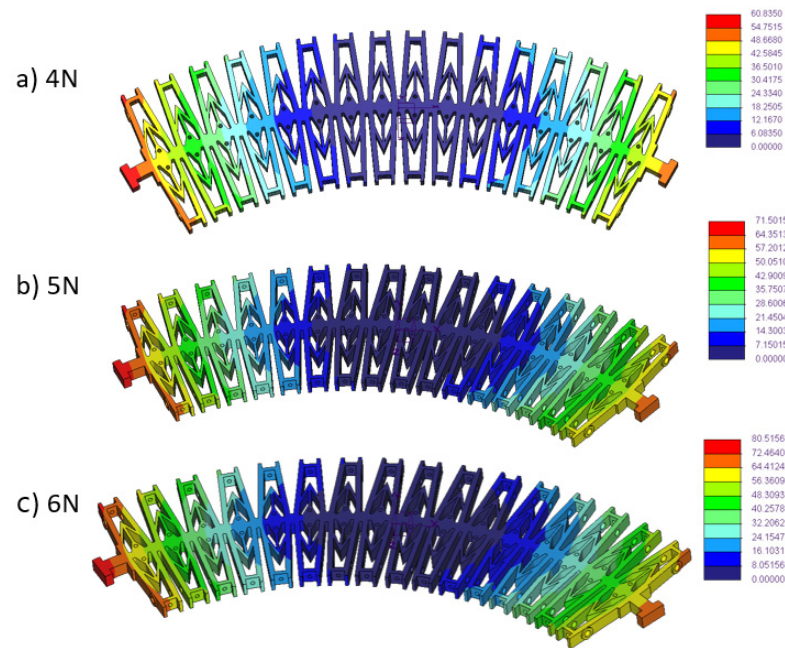


Figure 8. The displacement analysis [mm] of different rope tensions (4, 5, and 6 N).

Given that the robot track body was 3D printed using a TPU material, it was determined that the material's breaking strength exceeded the values obtained from the analysis. This demonstrates a successful outcome, as the ultimate tensile stress for TPU is 23.7 MPa in the xy plane. Figure 8 shows that a maximum displacement of 80 mm of the vertebral column ends can be obtained by applying a 6 N rope tension; however, this FEM model can provide only a rough estimation of the necessary steering force, since it evaluates only the elastic return force of the vertebral column, while many friction phenomena (rope–vertebral column, track–vertebral column, track–terrain) are neglected. As a consequence, the tests on the prototype are necessary for the complete evaluation of the structural behavior of the assembled robot.

4. Prototype Realization

The process of 3D printing begins with the creation of a 3D model of all the components using specialized Creo software. The models were then converted into STL files, which can be opened and adjusted in Cura software 4.1, and subsequently printed using an FDM machine. The Ultimaker S3 was utilized to print all the components of the robot. Due to the constraints of the 3D printer workspace, the main body was divided into two parts. The initial prototype of the vertebral column, depicted in Figure 8, was 3D printed using a TPU95A material from the Ultimaker company. Figure 9 displays the spinal column assembled alongside the white lateral supports, which were produced using an ABS material provided by the Ultimaker company. It has been used to experimentally evaluate the compliance along the different rotation directions. Figure 10 left represents the maximum lateral (yaw) flexion for the actuated steering. When the angle of rotation between the two end modules reaches 120° , the lateral supports on the internal side of the turn are in contact, and the turning radius is at its minimum (165 mm). Figure 10 right shows the pitch rotation for passive retroflexion, which is useful to adapt the robot shape to the terrain profile. Figure 11 shows the robot assembled with all the components except the track, while Figure 12 depicts the complete prototype of the Porcospino Flex. The track components (grey) are printed using an ABS material because of their high strength and favorable mechanical properties. The 3D printing parameters for all components are detailed in Table 1.

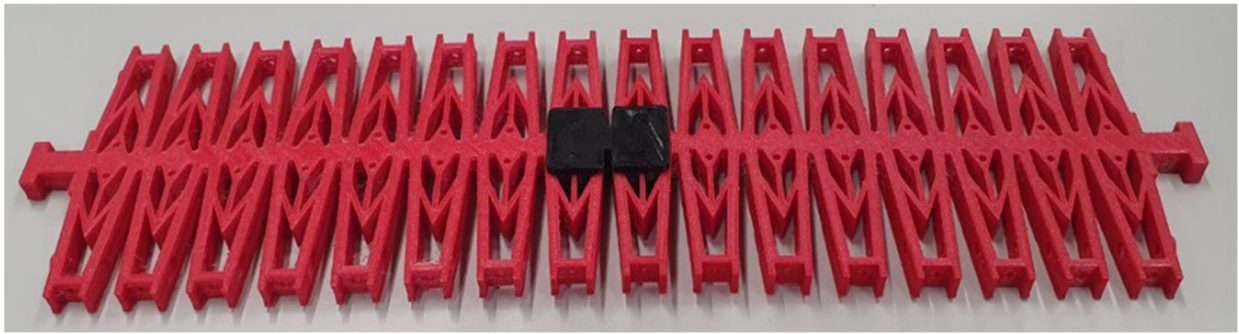


Figure 9. A 3D-printed prototype of the vertebral column.

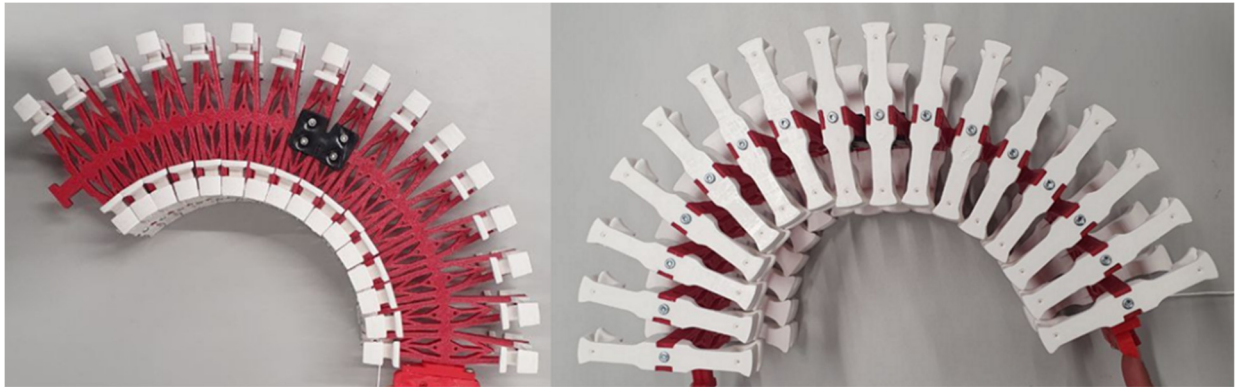


Figure 10. A prototype of the complete vertebral column (TPU in red and ABS in white): at its maximum yaw flexion (left) and maximum pitch flexion (right).

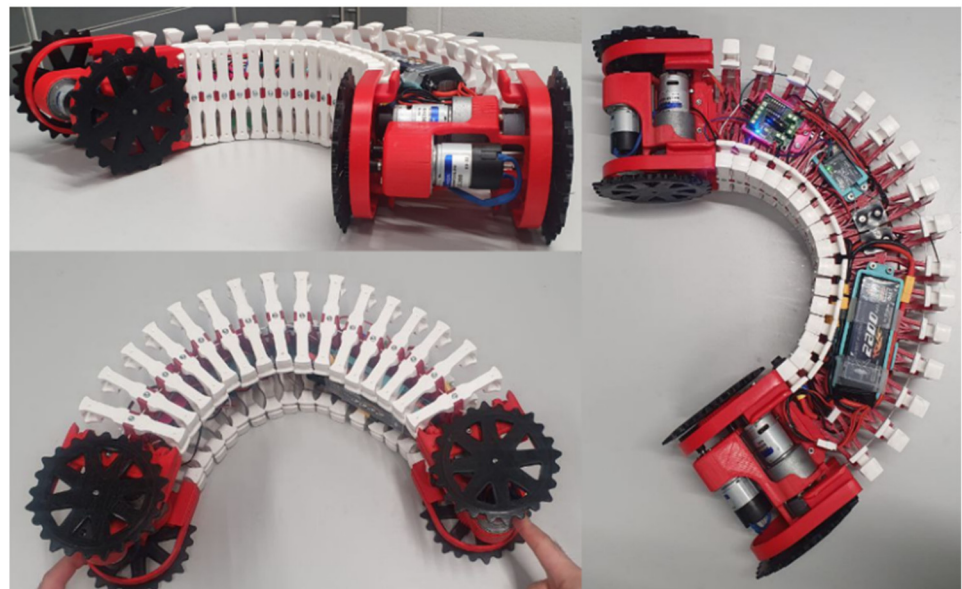


Figure 11. A prototype of the complete vertebral column (TPU in red and ABS in white): at its maximum yaw flexion (left) and maximum pitch flexion (right).

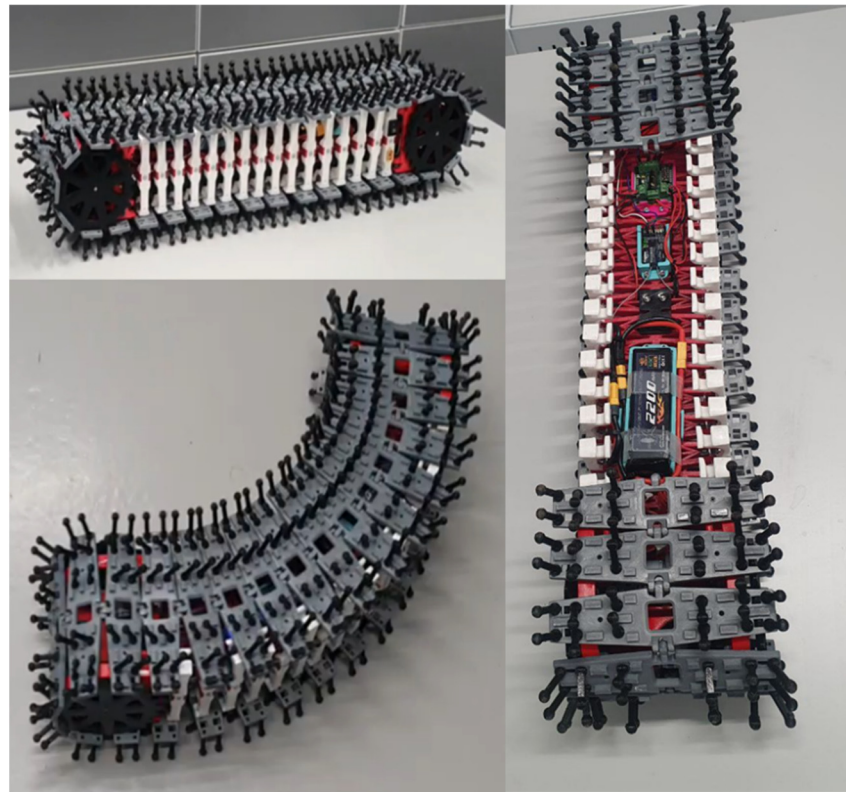


Figure 12. A prototype of the complete robot (**top left**), the robot with maximum pitch flexion (**down left**), and the complete robot with a partially opened track (**right**).

Table 1. The 3D printing parameters for the robot's components.

Parameter	Material	
	TPU 95A	ABS
Nozzle Temperature [°C]	225	245
Bed Temperature [°C]	25	85
Print Speed [mm/s]	25	60
Layer Height [mm]	0.15	0.15
Infill Density [%]	100	100

To control the robot's navigation, it was decided to adopt a Raspberry Pi 4B board with 8 GB of RAM, with the main features summarized in Table 2. The selected track actuators and steering actuators hosted in the end modules are Micromotors RH158 brushed gearmotors, with different reduction ratios (1:198.5 for the two TA and 1:243.8 for the two SAs); their features are listed in Table 3.

Table 2. The main features of the controller board.

Overall Dimension	85 × 56 mm
Processor	Broadcom BCM2711, quad-core Cortex-A72 (ARM v8) 64-bit SoC @ 1.5 GHz
Memory	8 GB
Video	2 × micro HDMI ports (up to 4Kp60 supported)
Connectivity	2.4 GHz and 5.0 GHz IEEE 802.11b/g/n/ac wireless
Power supply voltage	5V DC via USB-C/GPIO & PoE

Table 3. The main features of the TA and SA gearmotors.

Parameter	Rh158 200 (Track Actuator)	Rh158 250 (Steering Actuator)
Nominal voltage [V]	12	12
Length [mm]	69	69
Reduction ratio	198.5	243.8
Nominal torque [N·cm]	100	100
Speed at no load [rpm]	33	26
Speed at nominal torque [rpm]	23	21
Current at no load [mA]	140	140
Current at nominal torque [mA]	580	500
Input power [W]	7.0	6.0

5. Experimental Tests

At present, experimental tests are underway on the first prototype of the Porcospino Flex, which is operated remotely using radio control. These tests are instrumental in assessing the overall functionality of the proposed mechanical design and evaluating the robot’s ability to navigate uneven terrain by adapting to the environment using the passive retroflexion and torsion of the compliant vertebral column.

Figure 13 shows the Porcospino Flex climbing a square step with a height of 70 mm, exploiting the grasping of the spines in the first phase of the edge being overcome ($t = 1.0$ s) and the passive retroflexion of the compliant vertebral column during the whole maneuver. Figure 14 represents the robot climbing two steps with the same height of 70 mm placed at a distance of 215 mm. Figures 15 and 16 are related to tests in outdoor environments. In particular, Figure 15 illustrates a maneuverability test on grassy terrain, which is the most critical for steering due to the interactions between the spines and the grass, while Figure 16 shows the robot on asphalt, climbing the edge of a sidewalk with a height of 70 mm. The successful execution of the maneuvers in Figures 13–16 is shown in Ref. [40].

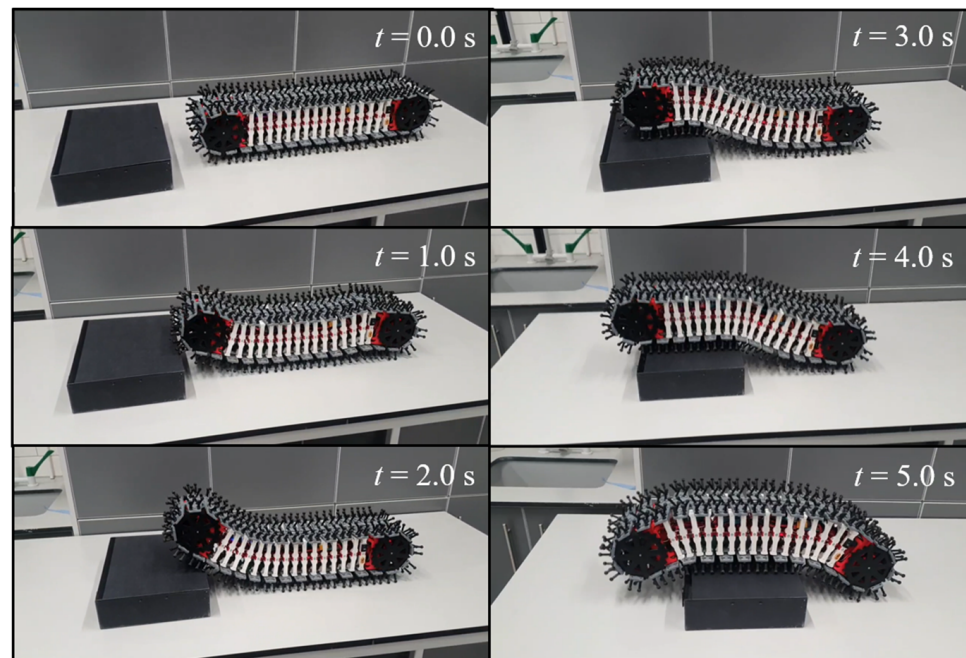


Figure 13. The Porcospino Flex climbing a single step with a height of 70 mm.

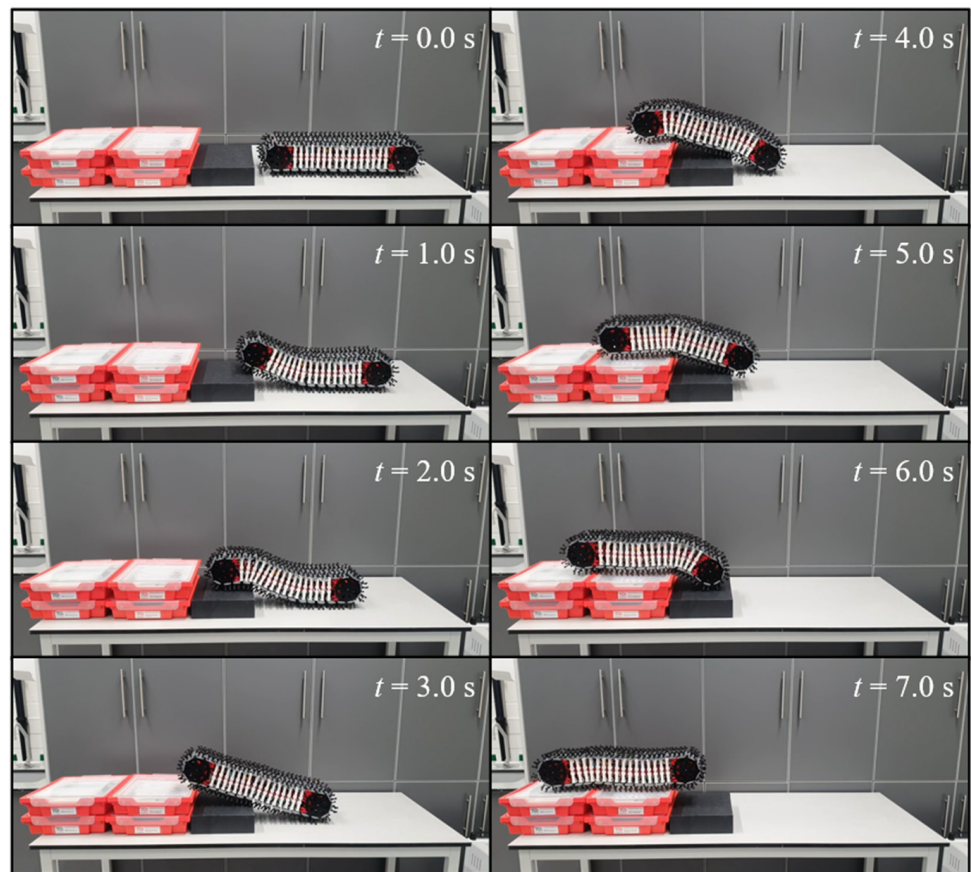


Figure 14. The Porcospino Flex climbing two successive steps with a height of 70 mm and a distance of 210 mm.



Figure 15. The Porcospino Flex in an outdoor test on a grassy irregular terrain.

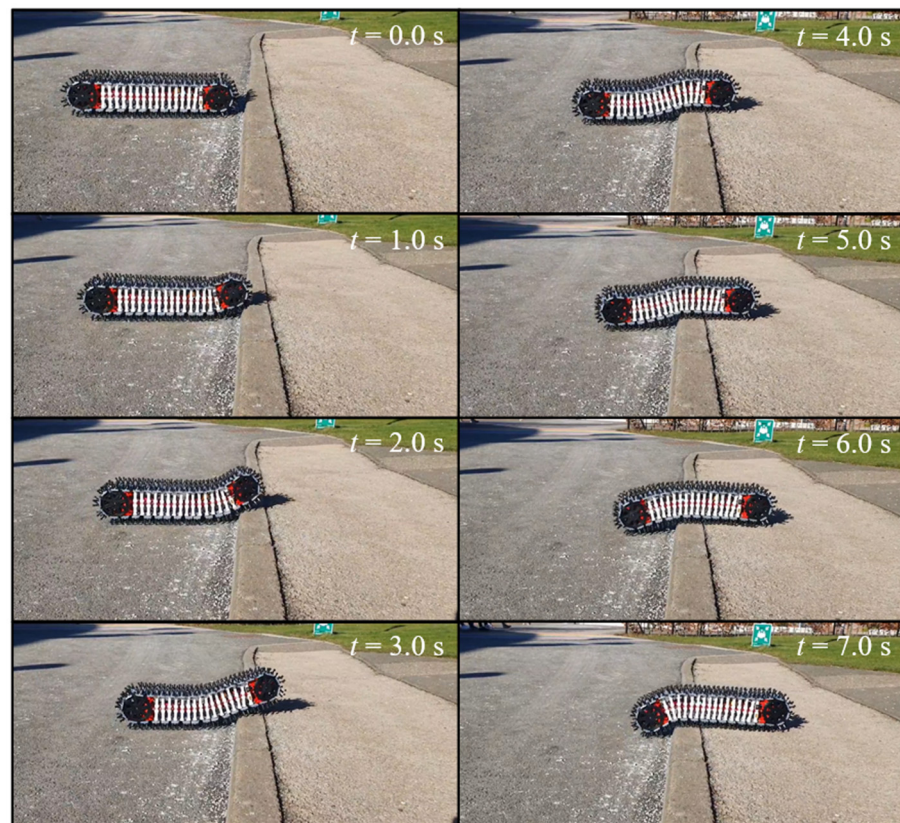


Figure 16. The Porcospino Flex in an outdoor test on asphalt, climbing a 70 mm sidewalk edge.

The Porcospino Flex's confirmed power drop of 2.134 W to 1.830 W, or of around 15% less, indicates a noticeable change from its previous version. Nonetheless, the acceleration's consistency is ascribed to the motor's fundamental qualities and design (0.131 m/s^2), which preserve stability even as the robot loses weight. These operating parameters lead to the establishment of the resulting speed at 0.16 rad/sec.

The Porcospino Flex represents a significant advancement in robot design, boasting a lighter construction compared to its predecessor. This weight reduction not only enhances its speed but also contributes to higher energy efficiency, marking a notable leap forward in performance. This achievement can be attributed to the streamlined subassembly, a testament to the continuous main body that sets this version apart from its forerunner. This structural refinement translates to heightened durability and stiffness, ensuring a robot that is more resilient and robust in its operations. The innovations in the Porcospino Flex lie in its adoption of a TPU vertebral column, as opposed to the previous model's reliance on an ABS material. This strategic material shift significantly reduces the likelihood of failures within the robot's framework, underlining meticulous attention to detail in enhancing its overall reliability.

The Porcospino Flex exhibits superior maneuverability, a trait attributed to both the flexibility of its chosen materials and the intricacies of its meta-structured design. These features work in tandem to enable the robot to navigate its surroundings with enhanced precision and agility, opening up new possibilities for applications in various environments. It demonstrates a more resource-conscious approach to material usage, marking a commendable step towards sustainability. This evolution in design not only contributes to a more efficient and effective robot but also aligns with a broader commitment to reducing environmental impact. Compared to the previous version, the guidance system's reliability for the track has been enhanced. This was achieved by redesigning the lateral supports and guiding pegs. The initial experimental tests have demonstrated the effectiveness of both the locomotion and steering mechanisms. Furthermore, the

heightened compliance of the vertebral column enables the robot to navigate through terrain irregularities and obstacles (as depicted in Figures 13, 14 and 16) without compromising the reliability of the redesigned track guidance system. You can also find the related video regarding the locomotion system of the robot in [40].

6. Conclusions

This paper explores the Porcospino Flex, an updated iteration of the Porcospino robot. This version is distinguished by its flexible spine. By incorporating a continuous meta-structure as the primary body and implementing a redesign, it was possible to decrease the robot's total weight from 4200 g to 3600 g. This also led to a reduced production time and cost. Additionally, the structural resilience to shocks was enhanced by eliminating bolted connections, which tend to introduce concentrated stresses. The track's guidance system reliability has been improved in comparison to the previous version. This was accomplished through the redesign of the lateral supports and guiding pegs. Both the locomotion and steering systems are improved and effective in the Porcospino Flex. Also, the flexibility of the robot's vertebral column allows it to maneuver through uneven terrain and obstacles.

The Porcospino Flex presents a versatile solution across multiple application scenarios, owing to its lightweight design and enhanced performance. Its reduced weight, achieved through a lattice structure, opens doors to agility and efficiency in demanding environments. In search and rescue operations, the robot maneuvers adeptly through debris and confined spaces, aiding in locating and rescuing survivors. Industrial inspections benefit from its flexibility and maneuverability, allowing access to intricate machinery and infrastructure. Moreover, in agricultural and environmental monitoring, the Porcospino Flex navigates uneven terrain with minimal impact, gathering crucial data without disturbance. Its lightweight construction further facilitates exploration in hazardous environments, ensuring safe navigation through challenging terrain. By addressing the pressing need for sustainability through reduced material usage and waste, the Porcospino Flex emerges as a pioneering solution poised to revolutionize various fields with its adaptability and eco-friendly design.

FEM was employed to analyze how the vertebral column behaves under various loads. The 3D printing technology known as FDM was utilized to manufacture all the parts of the robot. The assembly of the robot was reduced, and it was constructed using 3D-printed TPU and ABS with compliance distributed throughout. The robot's durability has been enhanced by utilizing less-rigid materials and opting for flexible TPU instead. The Porcospino Flex serves as an illustrative example of employing compliant mechanisms in robotics. This approach aims to streamline construction and minimize the quantity and weight of components. In terms of potential applications, the Porcospino Flex is well-suited for inspecting confined spaces that are challenging for humans or other robotic devices to access. This is due to its worm-like structure and the capacity to incorporate extra sensors along its vertebral column.

In summary, the Porcospino Flex stands as a testament to the relentless pursuit of innovation and excellence in robotics. Its lighter, more efficient build, coupled with its refined subassembly and novel material choices, combine to create a robot that is not only faster and more durable but also more environmentally conscious. With its heightened maneuverability and reduced material footprint, the Porcospino Flex represents a significant leap forward in the field of robotics, promising to pave the way for even more groundbreaking advancements in the future.

Author Contributions: Conceptualization, S.E.N., L.B. and M.B.; methodology, S.E.N., L.B. and M.B.; investigation and formal analysis, S.E.N., L.B., M.L.D., A.Z. and M.B.; resources, M.B. and L.B.; writing—original draft preparation, S.E.N., M.L.D. and L.B.; writing—review and editing, S.E.N., L.B., M.L.D., A.Z. and M.B.; supervision, M.B. and L.B.; funding acquisition, L.B. and M.B. All authors have read and agreed to the published version of the manuscript.

Funding: This research received no external funding.

Data Availability Statement: The original contributions presented in the study are included in the article. Further inquiries can be directed to the corresponding authors.

Conflicts of Interest: The authors declare no conflicts of interest.

References

- Nodehi, S.E.; Bruzzone, L.; Fanghella, P. SnakeTrack, A Bio-inspired, Single Track Mobile Robot with Compliant Vertebral Column for Surveillance and Inspection. *Mech. Mach. Sci.* **2022**, *120*, 513–520.
- Bruzzone, L.; Quaglia, G. Review article: Locomotion systems for ground mobile robots in unstructured environments. *Mech. Sci.* **2012**, *3*, 49–62. [[CrossRef](#)]
- Stückler, J.; Schwarz, M.; Schadler, M.; Topalidou-Kyniazopoulou, A.; Behnke, S. NimbRo Explorer: Semiautonomous Exploration and Mobile Manipulation in Rough Terrain. *J. Field Robot.* **2016**, *33*, 411–430. [[CrossRef](#)]
- Arvidson, R.E.; Iagnemma, K.D.; Maimone, M.; Fraeman, A.A.; Zhou, F.; Heverly, M.C.; Bellutta, P.; Rubin, D.; Stein, N.T.; Grotzinger, J.P.; et al. Mars Science Laboratory Curiosity Rover Megaripple Crossings up to Sol 710 in Gale Crater. *J. Field Robot.* **2017**, *34*, 495–518. [[CrossRef](#)]
- Rodinò, S.; Curcio, E.M.; di Bella, A.; Persampieri, M.; Funaro, M.; Carbone, G. Design, Simulation, and Preliminary Validation of a Four-Legged Robot. *Machines* **2020**, *8*, 82. [[CrossRef](#)]
- Mahapatra, A.; Roy, S.S.; Pratihari, D.K. Multi-Legged Robots—A Review. In *Multi-body Dynamic Modeling of Multi-legged Robots. Cognitive Intelligence and Robotics*; Springer: Singapore, 2020; pp. 11–32. [[CrossRef](#)]
- Tao, W.; Ou, Y.; Feng, H. Research on dynamics and stability in the stairs-climbing of a tracked mobile robot. *Int. J. Adv. Robot. Syst.* **2012**, *9*, 1–9. [[CrossRef](#)]
- Ugenti, A.; Galati, R.; Mantriota, G.; Reina, G. Analysis of an all-terrain tracked robot with innovative suspension system. *Mech. Mach. Theory* **2023**, *182*, 105237. [[CrossRef](#)]
- Quaglia, G.; Butera, L.G.; Chiapello, E.; Bruzzone, L. UGV epi.q-Mod. Mechanism and Machine Science. In Proceedings of the 20th CISM-IFTOMM Symposium on Theory and Practice of Robots and Manipulators, ROMANSY 2014, Udine, Italy, 7 April–7 July 2022; Volume 22, pp. 331–339.
- Arsenault, M.; Bergeron, Y.; Cadrin, R.; Legault, M.-A.; Millette, M.; Tremblay, M.-C.; Lepage, P.; Morin, Y.; Bisson, J.; Caron, S.; et al. Multi-Modal Locomotion Robotic Platform Using Leg-Track-Wheel Articulations. *Auton. Robot.* **2005**, *18*, 137–156. [[CrossRef](#)]
- Luo, Z.; Shang, J.; Wei, G.; Ren, L. A reconfigurable hybrid wheel-track mobile robot based on Watt II six-bar linkage. *Mech. Mach. Theory* **2018**, *128*, 16–32. [[CrossRef](#)]
- Bruzzone, L.; Baggetta, M.; Nodehi, S.E.; Bilancia, P.; Fanghella, P. Functional design of a hybrid leg-wheel-track ground mobile robot. *Machines* **2021**, *9*, 10. [[CrossRef](#)]
- Ma, N.; Zhou, H.; Yuan, J.; He, G. Comprehensive stiffness regulation on multi-section snake robot with considering the parasite motion and friction effects. *Bioinspiration Biomim.* **2024**, *19*, 016008. [[CrossRef](#)] [[PubMed](#)]
- Sun, L.; Wan, J.; Du, T. Fully 3D-printed tortoise-like soft mobile robot with multi-scenario adaptability. *Bioinspiration Biomim.* **2023**, *18*, 066011. [[CrossRef](#)] [[PubMed](#)]
- Divi, S.; Pierre, R.S.; Foong, H.M.; Bergbreiter, S. Controlling jumps through latches in small jumping robots. *Bioinspiration Biomim.* **2023**, *18*, 066003. [[CrossRef](#)] [[PubMed](#)]
- Bruzzone, L.; Nodehi, S.E.; Fanghella, P. Tracked Locomotion Systems for Ground Mobile Robots: A Review. *Machines* **2022**, *10*, 648. [[CrossRef](#)]
- Neumann, M.; Predki, T.; Heckes, L.; Labenda, P. Snake-like, tracked, mobile robot with active flippers for urban search-and-rescue tasks. *Ind. Robot.* **2013**, *40*, 246–250. [[CrossRef](#)]
- Liu, J.; Ma, S.; Lu, Z.; Wang, Y.; Li, B.; Wang, J. Design and experiment of a novel link-type shape shifting modular robot series. In Proceedings of the 2005 IEEE International Conference on Robotics and Biomimetics—ROBIO, Shatin, Hong Kong, 5–9 July 2005; pp. 318–323. [[CrossRef](#)]
- Hopkins, J.K.; Spranklin, B.W.; Gupta, S.K. A survey of snake-inspired robot designs. *Bioinspir. Biomim.* **2009**, *4*, 021001. [[CrossRef](#)] [[PubMed](#)]
- Haji, T.; Kinugasa, T.; Yoshida, K.; Amano, H.; Osuka, K. Experiment of maneuverability of flexible mono-tread mobile track and differential-type tracked vehicle. *Ind. Robot.* **2010**, *37*, 263–272. [[CrossRef](#)]
- Kislassi, T.; Zarrouk, D. A Minimally Actuated Reconfigurable Continuous Track Robot. *IEEE Robot. Autom. Lett.* **2019**, *5*, 652–659. [[CrossRef](#)]
- Nodehi, S.E.; Bruzzone, L.; Fanghella, P. Porcospino, spined single-track mobile robot for inspection of narrow spaces. *Robotica* **2023**, *41*, 3446–3462. [[CrossRef](#)]
- Wallin, T.J.; Pikul, J.; Shepherd, R.F. 3D printing of soft robotic systems. *Nat. Rev. Mater.* **2018**, *3*, 84–100. [[CrossRef](#)]
- Liu, Z.; Jiang, Q.; Zhang, Y.; Li, T.; Zhang, H.-C. Sustainability of 3D Printing: A Critical Review and Recommendations. In Proceedings of the ASME 2016 11th International Manufacturing Science and Engineering Conference, Blacksburg, VA, USA, 27 June–1 July 2016; Volume 2, pp. 1–8. [[CrossRef](#)]

25. Xu, Z.; Song, T.; Guo, S.; Peng, J.; Zeng, L.; Zhu, M. Robotics technologies aided for 3D printing in construction: A review. *Int. J. Adv. Manuf. Technol.* **2022**, *118*, 3559–3574. [[CrossRef](#)]
26. Zadpoor, A.A. Additively manufactured porous metallic biomaterials. *J. Mater. Chem. B* **2019**, *7*, 4088–4117. [[CrossRef](#)] [[PubMed](#)]
27. Helou, M.; Kara, S. Design, analysis and manufacturing of lattice structures: An overview. *Int. J. Comput. Integr. Manuf.* **2018**, *31*, 243–261. [[CrossRef](#)]
28. Sun, Y.; Lueth, T.C. Enhancing Torsional Stiffness of Continuum Robots Using 3-D Topology Optimized Flexure Joints. *IEEE/ASME Trans. Mechatron.* **2023**, *28*, 1844–1852. [[CrossRef](#)]
29. Filipov, E.T.; Tachi, T.; Paulino, G.H. Origami tubes assembled into stiff, yet reconfigurable structures and metamaterials. *Proc. Natl. Acad. Sci. USA* **2015**, *112*, 12321–12326. [[CrossRef](#)] [[PubMed](#)]
30. Zhou, X.; Ren, L.; Song, Z.; Li, G.; Zhang, J.; Li, B.; Wu, Q.; Li, W.; Ren, L.; Liu, Q. Advances in 3D/4D printing of mechanical metamaterials: From manufacturing to applications. *Compos. Part B Eng.* **2023**, *254*, 110585. [[CrossRef](#)]
31. Chen, Y.; Mai, Y.-W.; Ye, L. Perspectives for multiphase mechanical metamaterials. *Mater. Sci. Eng. R Rep.* **2023**, *153*, 100725. [[CrossRef](#)]
32. Saxena, K.K.; Das, R.; Calius, E.P. Three Decades of Auxetics Research—Materials with Negative Poisson’s Ratio: A Review. *Adv. Eng. Mater.* **2016**, *18*, 1847–1870. [[CrossRef](#)]
33. Singh, R.; Agarwal, A.; Anthony, B.W. Design of optical meta-structures with applications to beam engineering using deep learning. *Sci. Rep.* **2020**, *10*, 19923. [[CrossRef](#)]
34. Wang, L.B.; Wang, C.; Lei, Y.Z.; Yang, S.K.; Wu, J.H. Broadband high-efficiency meta-structures design by acoustic critical absorption effect. *Appl. Acoust.* **2022**, *200*, 109063. [[CrossRef](#)]
35. Dikici, Y.; Jiang, H.; Li, B.; Daltorio, K.A.; Akkus, O. Piece-By-Piece Shape-Morphing: Engineering Compatible Auxetic and Non-Auxetic Lattices to Improve Soft Robot Performance in Confined Spaces. *Adv. Eng. Mater.* **2022**, *24*, 2101620. [[CrossRef](#)]
36. Kelkar, P.U.; Kim, H.S.; Cho, K.-H.; Kwak, J.Y.; Kang, C.-Y.; Song, H.-C. Cellular Auxetic Structures for Mechanical Metamaterials: A Review. *Sensors* **2020**, *20*, 3132. [[CrossRef](#)] [[PubMed](#)]
37. Ma, R.; Bi, K.; Hao, H. Inerter-Based Structural Vibration Control: A State-of-the-Art Review. *Eng. Struct.* **2021**, *243*, 112655. [[CrossRef](#)]
38. Waterworth, S.A.K. How to Get Rid of Millipedes in the House. *Forbes*. Available online: <https://www.forbes.com/home-improvement/pest-control/how-to-control-centipedes-millipedes/> (accessed on 24 December 2023).
39. Charles. 10 Fascinating Facts about Monotremes. Available online: <https://earthlyuniverse.com/10-fascinating-facts-monotremes/> (accessed on 24 December 2023).
40. Porcospino 2 (Flex). Available online: <https://www.youtube.com/watch?v=SS7fUyP8bMU> (accessed on 3 May 2024).

Disclaimer/Publisher’s Note: The statements, opinions and data contained in all publications are solely those of the individual author(s) and contributor(s) and not of MDPI and/or the editor(s). MDPI and/or the editor(s) disclaim responsibility for any injury to people or property resulting from any ideas, methods, instructions or products referred to in the content.